Spatio-Temporal Structuring of Brain Activity — Description of Interictal EEG in Paediatric Frontal Lobe Epilepsy

W. Bunk[1*], T. Aschenbrenner[1], G. Kluger[2] and S. Springer[3]

1) Max-Planck-Institut für extraterrestrische Physik, Giessenbachstrasse, 85748 Garching, Germany. 2) Klinik für Neuropädiatrie, Epilepsiezentrum, D-83569 Vogtareuth, Germany. 3) Heckscher-Klinikum für Kinder- und Jugendpsychiatrie und Psychosomatik, München; Kinderklinik und Poliklinik im Dr. von Haunerschen Kinderspital, Klinikum der Universität München, Germany.

*) Tel.: +49-89-30000-3548, Fax: +49-89-30000-3390, E-mail: whb@mpe.mpg.de

Running Title: Spatio-Temporal Structuring of Brain Activity

Abstract

A method for the quantitative assessment of spatio-temporal structuring of brain activity is presented. This approach is employed in a longitudinal case study of a child with frontal lobe epilepsy (FLE) and tested against an age-matched control group. Several correlation measures that are sensitive to linear and/or non-linear relations in multichannel scalp EEG are combined with an hierarchical cluster algorithm. Beside a quantitative description of the overall degree of synchronization the spatial relations are investigated by means of the cluster characteristics. The chosen information measures not only demonstrate their suitability in the characterization of the ictal and interictal phases but they also follow the course of delayed recovery of the psychiatric symptomatology during successful medication. The results based on this single case study suggest testing this approach for quantitative control of therapy in an extended clinical trial.

Key terms: hierarchical cluster algorithm, information measures, spatio-temporal structuring, synchronization, quantitative control of therapy

1 Introduction

In the last decade synchronization processes in the brain were put in the focus of neurological science. They are claimed to be responsible for a variety of essential properties of the brain: Synchronization is supposed to be a fundamental method of information coding in the brain [1] e.g. in visual perception. Obviously, in epileptic seizures synchronization plays an important role and its quantitative description is relevant for diagnostic purposes ([2]–[4]). As the number of neurons involved in this synchronized activity is rather high the associated surface EEG often shows typical epileptiform patterns (spikes, waves) with considerable amplitudes. In interictal periods these typical epileptic EEG patterns are often missing which does not contradict the diagnosis of epilepsy [5]. Fingelkurts et al. [6] hypothesize that chronic epilepsy changes the brains state even in interictal periods displaying altered anatomical, biochemical and functional properties. They claim that the interictal EEG, even without epileptiform abnormalities, has a number of characteristic differences from the EEG of healthy subjects and "*a therapeutic intervention could aim to restore the actual composition of brain oscillations and their temporal behavior, similar to those of the normal EEG*" [6]. Hence, an important aspect of interictal EEG assessment is the evaluation of spatio-temporal synchronization. Up to now the analysis of synchronization is not viewed as a standard method for diagnosing epilepsy based on interictal EEGs [5]. We present in this paper a methodology to quantify synchronization properties of brain activity. A number of linear and non-linear synchronization measures are employed to test for their suitability in this question.

Frontal lobe epilepsy FLE is a common type of extra-temporal epilepsy in adults. In childhood, however, only less than 10% of the developed (extra-temporal) epilepsy syndromes are of this form [7]. Because of the considerable cognitive

and behavioral deficits associated with FLE, anti-epileptic therapy is of greatest importance from the very beginning of the disease.

For a comprehensive diagnosis clinical signs, neuropsychological assessments, electroencephalographic findings, and magnetic resonance images have to be considered in a synoptic view. The anatomical assignment of clinical syndromes is controversial for FLE [8]. Due to the variable and rapid spread of the epileptic activity the seizure characteristics can vary strongly [9]. Seizures with origin in the frontobasal cingulate area often include complex motor automatisms [8]. Common and striking clinical features related to FLE especially in children are atypical absences and psychomotor seizures, characterized by complex (organized) movements of the limbs and an increased general motor activity ([10],[11]). Seizures originating from the frontal lobe are usually of short duration, frequent, and often arise during sleep [10]. The onset of the FLE in childhood is very frequently misdiagnosed as sleep disorder or as a psychogenic seizure ([9],[12],[13]). Neuropsychological testing and assessments regarding behavioral deficits such as increasing learning disability and forgetfulness give further indications on the status during the ongoing disease ([14]–[16]). The observed behavioral disorders are explained by the frequent subclinical epileptic activity in the prefrontal area visually detectable only with intracranial EEG recordings [12].

The ictal electroencephalographic monitoring of FLE patients yields typical features of epileptic discharges in general, e.g. low-amplitude-fast-activity, rhythmic spikes and waves [12]. Particularly, one observes ictal and pre-ictal synchronization effects over wide areas of the brain. In the interictal phase the scalp-EEG is mostly normal, i.e. by means of a conventional visual inspection suspicious features can hardly be found. Even from the ictal EEG, it is often difficult to distinguish between FLE and temporal epilepsy [17]. For a more precise localization of the epileptic focus an ictal and intracranial recording is

needed. Because of the rapid spread of the pathological patterns the origin of the epileptic discharge is hard to detect even with invasive techniques.

The objective of this paper is to present a methodological approach to the analysis of scalp electrode EEG for a characterization of spatio-temporal structuring of brain activity.

The paper is organized as follows:

Section 2 gives a description of the data together with a clinical history of the patients and some technical aspects of the electroencephalographic data acquisition. In section 3 follows an detailed explanation of our methodological approach for the study of brain synchronization. It comprises the definition of the various correlation measures used in frequency and time domain, the derived similarity measures and the hierarchical clustering approach. Section 4 presents our quantitative results and introduces a visualization of the cluster behavior by a two-dimensional projection onto the head surface. The paper ends with a short summary of the results. Main emphasis is placed in the discussion on the observed specific spatio-temporal structuring in the patient with FLE.

2 Patients and Data

2.1 Patients

In this study the single case results of the analysis of several EEG recordings covering two years of a child (patient A) are compared with the outcome of an age-matched control group.

Patient A has a family history of epilepsy. Until the age of eleven years the boy's motor and cognitive development was in the normal range. The paediatric and neurological investigation never showed pathological results. At 11.5 years the boy suffered from atypical absences with enuresis but without spasms. The absences were followed by complex partial seizures (11.6 years). At the age of

11.8 years frequent typical hypermotoric seizures appeared. Since this time his psychopathological status deteriorated rapidly: The boy became disorientated and aggressive. Other clinical features of his aggravated status were speech disorders, extremely shortened attention span, reduced emotional control, motor hyperactivity and depressive mood. These clinical manifestations and the findings from the EEG recordings (spike waves, low-amplitude-fast-activity during seizures) are consistent with the diagnosis of a frontal lobe epilepsy generated in the frontobasal area. MRI of the brain, laboratory diagnostic of serum, and CSF were inconspicuous.

Regular medication started at the age of 12.1 years with oxcarbazepine (15 mg/kg/d), which induced a first status epilepticus. This medication was immediately stopped and replaced by high dose i.v.-valproic acid and i.v.-phenobarbital. At 12.15 years it was possible to obtain seizure freedom with valproic acid (22 mg/kg/d) and lamotrigine (5 mg/kg/d). Half a year after the beginning of the medication (12.7 years) reduced cognitive capability with learning disability (IQ 85) was measured using Raven Test.

As a consequence of dose reduction atypical absences occurred again at the age of 12.5 to 12.9 years (not documented by EEG) which required increased lamotrigine doses. The boy is seizure free since the age of 14.0 years with an ongoing lamotrigine monotherapy.

Patient A had an unsuspicious occipital background activity within the alpha-band. This background activity, assessed by visual EEG inspection in interictal phases, did not change significantly during the disease. The first four EEG, which entered this study, are taken at an age of 12.1 years and cover the first month of medical therapy (acute phase). In the first EEG a seizure was derived. Pre-ictal, a short episode of generalized low-amplitude-fast-activity was recorded. During seizure (one minute) rhytmic spike wave complexes were seen as most prominent ictal patterns. In the course of the second EEG recording

another seizure episode occured. Starting at $t \approx 6.7\ min$ (compare figure 1), epileptic activity persisted with rhythmic generalized delta activity most pronounced in frontal areas. The EEG seizure patterns were similar to the first attack. During the following six EEG recordings no seizure took place. Until the age of 12.1 years typical interictal bifrontal epileptiform patterns (like spikes and spike wave complexes) were detected visually. The third and the fourth EEG showed only sporadic atypical irregular sharp waves. The subsequent four EEG were obtained at an age of 13.15, 13.35, 13.73 and 13.96 years. These four EEG recordings (including the one during clinical deterioration at 13.15 years) showed no epileptiform patterns. The EEG recordings span a period of almost two years of successful therapy.

The age-matched control group consists of three patients whose EEG recordings cover an age range from 10.6 to 14.4 years. Patient B_1 of this group was diagnosed with an uncomplicated generalized epilepsy. He suffered from three unprovoked generalized seizures before starting treatment and is seizure-free with a monotherapy of valproic acid. The patients B_2 and B_3 experienced only one unprovoked generalized epileptic seizure. Ten EEG were taken from patient B_1 (10.6 to 13.8 years) and one EEG from B_2 (11.3 years) and B_3 (14.4 years), respectively. All EEG recordings of the control group were classified as normal. These three patients showed seizure freedom for more than five years of follow-up. In contrast to patient A their cognitive and emotional development was in the normal range. In this sense it was an unbiased selection of controls matching the age of patient A.

2.2 Data

The positioning of the electrodes followed that of the standardized 10-20–International System of Electrode Placements. Every EEG recording consists of 21

synchronously obtained time series. Our data base is made up by a number of twenty multichannel EEG recordings: Eight EEG are recorded from patient A (age range 12.06–13.96 y). Twelve EEG are derived from the control group (three patients, age range 10.61–14.37 y). Every EEG record measures brain activity for at least 10 minutes at a sampling rate of 250 Hz and a signal depth of 16 bits. Information about patients and EEG recordings are listed in table 1. To guarantee the comparability, the patients state during EEG monitoring was classified with a time resolution of one second by an expert. Components of the patients state assessed were e.g. vigilance, attention level, artefacts (movements) and epileptic activity. This expert was not directly involved in the subsequent analysis. The selected EEG-segments (free of artefacts and movements, awake, same level of attention, no interictal epileptiform discharges or ictal EEG patterns) form a homogenous data base which enters the study.

3 Methods

To obtain a time dependent characterization of brain activity the data has been analyzed with a sliding window technique. Since the window size n_0 at a given sampling rate determines the frequency bandwidth we chose $n_0 = 512$, corresponding to a real time period of slightly more than two seconds. The consecutive windows overlap by half the window size, which results in more than 900 separate windows for a typical EEG recording of 15 minutes and a time resolution of $\sim$1.0 seconds.

To describe the spatio-temporal cluster properties, at each instant of time t (center of window) several correlation measures between data of the several leads were computed. From the respective quantity appropriate distance measures were derived. Finally, the resulting distance matrices were evaluated in a cluster

Patient/ Group		ΔT [s]	Age [y]	State of Vigilance	Seizure during EEG	Seizure Freedom [h]	Medication	Clinical Diagnosis	EEG Findings
A	SC/acute phase	710/125	12.060	AW/SL	+	< 1	OXC	FLE – mult. seizures	SW frontal + seizure patterns
	SC/acute phase	940/340	12.096	AW	+	< 1	VPA + LTG	FLE – seizures	SW frontal + seizure patterns
	SC/acute phase	3600/769	12.104	AW/SL	–	> 24	VPA + LTG	FLE – only atyp. absences	sporadic SW
	SC/acute phase	990/932	12.159	AW	–	> 100	VPA + LTG	FLE – seizure free	sporadic SW
	SC	900/435	13.151	AW	–	> 100	VPA + LTG	FLE – seizure free	inconspicuous
	SC	970/921	13.351	AW	–	> 1800	VPA + LTG	FLE – seizure free	inconspicuous
	SC	930/615	13.729	AW	–	> 5100	VPA + LTG	FLE – seizure free	inconspicuous
	SC	980/648	13.964	AW	–	> 7200	LTG	FLE – seizure free	inconspicuous
B_1	CG	890/761	10.608	AW	–	> 24	NoMed	after 1. unprovS	inconspicuous
	CG	1900/588	10.877	AW/SL	–	> 24	NoMed	after 2. unprovS	inconspicuous
	CG	660/583	10.918	AW	–	> 380	NoMed	after 2. unprovS	inconspicuous
	CG	1680/544	11.301	AW/SL	–	> 3700	NoMed	after 2. unprovS	inconspicuous
	CG	900/782	11.323	AW	–	> 3900	NoMed	after 2. unprovS	inconspicuous
	CG	1030/785	11.858	AW/SL	–	> 100	NoMed	after 3. unprovS	inconspicuous
	CG	1030/856	11.929	AW/SL	–	> 700	VPA	GE – seizure free	inconspicuous
	CG	960/944	12.299	AW	–	> 3900	VPA	GE – seizure free	inconspicuous
	CG	900/824	12.792	AW	–	> 8200	VPA	GE – seizure free	inconspicuous
	CG	880/755	13.751	AW	–	> 16600	VPA	GE – seizure free	inconspicuous
B_2	CG	900/879	11.282	AW	–	> 24	NoMed	after 1. unprovS	inconspicuous
B_3	CG	930/841	14.373	AW	–	> 24	NoMed	after 1. unprovS	inconspicuous

Table 1: *Description of patients and data. Abbreviations: SC: Single Case, CG: Control Group; ΔT: Length of recording/duration of selected EEG-segments according to the definitition in section 2.2; AW: awake, SL: sleep (periods during sleep were skipped in the analysis); NoMed: no medication, OXC: oxcarbazepine, VPA: valproic acid, LTG: lamotrigine; FLE: frontal lobe epilepsy, GE: generalized epilepsy, unprovS: unprovoked seizure; SW: sharp waves.*

analysis in analogy to Bonanno et al. [18] (later adopted in the context of EEG-analysis by Aschenbrenner et al. [19] and Lee et al. [20]).
Details of this procedure are explained in the following subsections.

3.1 Correlation and Distance Measures

The correlation between each pair of time series was estimated in several ways. Hereby, we distinguish between measures in the frequency domain (using Fourier transform) and time domain when applying correlation algorithms directly to the time series. In the latter case we particularly studied the differences between linear and non-linear correlation measures.

3.1.1 Correlation Measures in the Frequency Domain

Fourier transform is applied to succeeding data segments (n_0 data points), generated by the sliding window procedure and using window sampling techniques (Hamming windowing). For further analysis the normalized power spectra $F_t^X(\nu_i)$ of each window of time series X were taken, considering only the spectral range between $0 \leq \nu_i \leq 30\ Hz$, so that $\sum_{\nu_i=0}^{30Hz} F_t^X(\nu_i) = 1$.
The "correlation" between spectra of X and Y was then estimated by means of the *Kullback-Leibler entropy* [21]:

$$E_t^{KL}(X,Y) = \sum_{\nu_i=0}^{30Hz} F_t^X(\nu_i) \log_2 \left(\frac{F_t^X(\nu_i)}{F_t^Y(\nu_i)} \right) \tag{1}$$

The Kullback-Leibler entropy measures the dissimilarity between two statistical distributions based on a generalization of Shannon's definition of information entropy. Since $E_t^{KL}(X,Y)$ is usually not symmetric, we symmetrized $E_t^{KL}(X,Y)$ according to the "resistor-average distance" [22]:

$$d(E_t(X,Y)) = d(E_t(Y,X)) = \left(\frac{1}{E_t^{KL}(X,Y)} + \frac{1}{E_t^{KL}(Y,X)} \right)^{-1} \tag{2}$$

In this modified form, the symmetrized Kullback-Leibler entropy can serve as a kind of a distance measure: $d\left(E_t\left(X,Y\right)\right)=0$ iff $F^X(\nu_i)=F^Y(\nu_i)\forall\nu_i$, it is >0 else. This measure emphasizes similarities in the spectral content of both time series while phase aspects are ignored.

3.1.2 Correlation Measures in the Time Domain

To quantify synchronization between pairs of time series X and Y with respect to their temporal behavior some correlation measures are tested. The most common measure is *Pearson's coefficient of correlation*:

$$\rho_t\left(X,Y\right)=\frac{\sum_{i=0}^{n_0-1}(X_i-\overline{X})(Y_i-\overline{Y})}{\sqrt{\sum_{i=0}^{n_0-1}(X_i-\overline{X})^2\sum_{i=0}^{n_0-1}(Y_i-\overline{Y})^2}} \tag{3}$$

Even so ρ is independent of the origin and the scale it assumes a mutual linear correlation between X and Y, and normality of the distributions. In order to overcome this restrictions, the *Spearman rank-order correlation coefficient* can be used:

$$\rho_t'\left(X,Y\right)=1-6\frac{srd}{n_0(n_0^2-1)}. \tag{4}$$

In this expression srd denotes the sum of the squared difference in the rank ordering of the corresponding variables X and Y. This distribution-free correlation measure is not restricted to linear correlations and is robust with respect to the outlier-problems in time series.

We focus, however, on the use of an information based correlation measure, the mutual information M. Its definition is closely related to Shannon's information entropy H.

$$M_t\left(X,Y\right) \quad = \quad \sum_{i=0}^{nb-1}\sum_{j=0}^{nb-1} p_t(X_iY_j)\log_2\frac{p_t(X_iY_j)}{p_t(X_i)p_t(Y_j)} \tag{5}$$

$$= \quad H_t(X) + H_t(Y) - H_t(X,Y) \tag{6}$$

Herein, $H_t(X) = -\sum_{i=0}^{nb-1} p_t(X_i)\ log_2\ p_t(X_i)$ is the so-called marginal entropy, i.e. Shannon's information entropy applied to X. The mixed term $H_t(X,Y)$ in Eq. 6 is called joint entropy. nb gives the number of discrete bins of the corresponding distribution functions $p_t(X)$ and $p_t(Y)$. The discretization of X and Y has not to be homogeneous.

If we calculate the mutual information for every pair of EEG recordings we end up with a symmetric mutual information matrix $\widehat{M}$. Major differences to the correlation coefficients of Pearson and Spearman are that the mutual information does not distinguish between positive and negative correlations and that it is less sensitive to phase shifts between the data sets.

3.2 Similarity and Dissimilarity Measures

As similarity measures (e.g. correlation coefficient, mutual information) are never metric [23] for clustering purposes these measures have to be transformed to dissimilarity metric measures ("distances"). All measures of correlation Q can be transformed to an appropriate distance matrix $\widehat{D}$ with elements $d(Q_t(X,Y))$ that allows for the investigation of similarity clustering. In the case of Pearson's coefficient, we follow the proposal of Bonanno et al. [18]. The distance measure for each epoch t is given by

$$d(\rho_t(X,Y)) = \sqrt{2(1-\rho_t)}. \tag{7}$$

$d(\rho)$ takes values between 0 (perfectly correlated, $\rho = 1$) and $\sqrt{2}$ (perfectly anti-correlated, $\rho = -1$).

For Spearman's coefficient, the distance measure is given by the equivalent expression. $d(\rho)$ and $d(\rho')$ fulfill the requirements of a metric[1].

[1] A metric is a symmetric, positive quantity — minimal value 0 achieved for identical elements —, which meets the triangle inequality [23].

In the case of the mutual information we use as a distance measure

$$d\left(M_t\left(X,Y\right)\right) = \log_2 nb - M_t\left(X,Y\right). \tag{8}$$

The Kullback-Leibler entropy is a dissimilarity (distance-like) measure by definition and therefore a further transformation is not necessary. Even the symmetrized version of the Kullback-Leibler entropy (see Eq. 2) is non-metric in a rigid sense as it still violates the triangle inequality. However, the application of the Kullback-Leibler entropy in the framework of section 4.1 does not require metricity.

3.3 Hierarchical Clustering

For the description of the overall relationship between the EEG measurements at the different locations in form of an indexed tree we apply a single linkage cluster analysis SLCA [24]. The definition of the respective hierarchy $H = \{h_0, h_1, ...\}$ is based on the interobject dissimilarities derived from the correlation measures as shown in the previous section.

Given a distance measure $d\left(Q_t\left(X,Y\right)\right)$ (e.g. in form of a distance matrix) the reconstruction of a hierarchical tree in the sense of a SLCA approach is straight forward with the help of the so-called minimum spanning tree (MST) [24]. One possible way of the reconstruction of a hierarchical tree is briefly summarized here (for details see [24] or [25]):

In the first step of generating the hierarchy, the minimum spanning tree has to be constructed. Remember, for a number n of objects the MST is the shortest connection of all these objects without any loops and it consists of $n-1$ edges e_{ij}. (Most algorithms for generating the MST are based on the concepts of Kruskal [26] or Prim [27].) The resulting tree is represented by a sequence of edges $\{e_{ik}, ..., e_{lj}\}$. Hereby, the length of edge e_{ik} is equivalent to the distance d_{XY} as introduced in the previous section. The ultrametric distance d^*_{XY} be-

tween two arbitrary elements X and Y is then given by the longest edge of the sequence $\{e_{Xk}, ..., e_{lY}\}$ that connects the vertex X with the vertex Y along the tree.

The process of generating a hierarchical tree can be understood as an iterative splitting process, starting at the highest aggregation level at which all elements belong to the same hierarchy h_0. At this level $f(h_0)$ is the maximum value of $d^*\left(Q_t\left(X, Y\right)\right)$. At the next (lower) level the set of elements is divided into these two sets that are separated by the longest ultrametric distance. By construction, this is a realization of the SLCA-approach, guaranteeing that the distance between two clusters equals the minimum intercluster distance between arbitrary elements of these clusters. This iterative procedure is repeated with ever decreasing thresholds (ultrametric distances) of the generated subtrees from top to bottom until $f(h_k) = 0$, indicating that the resulting hierarchy consist only of one element.

We want to emphasize that other approaches than the SCLA method could be chosen for the agglomerative algorithm, e.g. by applying complete linkage distances or the use of the distances between cluster centroids. In this context, however, we explicitly decided for this approach because it is adequate for the description of the dynamical propagation of brain activities between distant areas.

The left panel in figure 4, 5 and 6, respectively, shows a visualization of the corresponding hierarchical tree. The numerical aggregation levels, equivalent to the defined cluster distances, are drawn at the ordinate.

4 Results

Applying the described techniques to EEG recordings, we obtain a time-resolved information on spatial characteristics of electrical brain activity. In a first step,

however, the analysis considers the overall level of synchronization — ignoring time-dependence and local information — in the different patients and EEG recordings. We investigated whether such global measures are able to distinguish between the single case and the control group even in long lasting interictal periods. Finally, we focus on the results from the clustering procedure, which yields spatio-temporal characteristics of brain activity. Locally resolved properties of the processes provide further details to characterize brain activity and furthermore could give some hints on the localization of pathologies.

4.1 Temporal Characterization

For every epoch (window) labeled with index t we calculated the distance matrix d_t based on the respective similarity measure Q as defined in section 3.2. The mean of all entries of the distance matrix for each epoch t yields a new measure $\overline{d\left(Q_t\right)}$ that quantifies the general degree of synchronization at each time t, whilst the spatial information is not yet considered here explicitly. Figure 1 displays the time course of $\overline{d\left(M_t\right)}$, i.e. the distance measure using the mutual information, for the second record of patient A. Note, that in the segment prior to seizure the distant values are significantly lower than in the control group. At $t \approx 6.7\ min$ starts a psychomotor seizure, which is reflected by a significantly decreased value of $\overline{d\left(M_t\right)}$: Apparently, the transition to seizure (marked by the gray background) coincides with a sharp rise and drop in the distance measure, indicating a short-time desynchronization followed by a persistent higher degree of synchronization.

In order to characterize the degree of synchronization between all 21 lead-areas of the multi-channel EEG for each patient and each record, we average over the spatial mean: $D\left(Q\right) = \frac{1}{T}\sum_{i=1}^{N}\overline{d\left(Q_i\left(X,Y\right)\right)}$. The according standard deviation is abbreviated by $\sigma_D\left(Q\right)$. We observe significant differences between patient A (acute phase) and the control group in the sense that the correlation distances

are smaller in general. However, this effect is most distinctive by using either the spectral description in the frequency domain combined with the non-linear similarity measures (according to Eq. 2) or by use of the non-linear correlation measure, namely the mutual information (see Eqs. 6 and 8).

Moreover, the diagrams in figure 2 and 3 show that these obvious differences vanish during treatment and with time quite monotonically. This trend is obvious in both non-linear measures, using Kullback-Leibler distance of Fourier spectra (see figure 2) or the distance measure based on the mutual information displayed in figure 3. This normalization of the overall level of synchronization is in parallel with the improvement of the psychiatric status.

The clustering behavior using mutual information yields systematic lower values for patient A — at least in the first three recordings — which express a higher similarity between the signals of the various channels compared to that of the control group. The results from the fourth and the following recordings are comparable to those of the control patients. Figure 3 shows the evolution of patient A under treatment using mutual information distance $D(M)$.

The discriminative power of a distance measure $D(Q)$ between two groups "0" and "1" is expressed by

$$Contrast = \frac{\left(D^1(Q) - D^0(Q)\right)^2}{\left(\sigma_D^1(Q)\right)^2 + \left(\sigma_D^0(Q)\right)^2} \tag{9}$$

Table 2 lists this contrast parameter between acute phase of patient A on one side ("0") and control group B ("1") on the other side for the several derived measures.

The highest contrast in synchronization between these groups is achieved by Kullback-Leibler distances of the power spectra ($Contrast = 3.25$, see figure 2), followed by mutual information ($Contrast = 1.42$, see figure 3). It is remarkable that Spearman's rank coefficients of correlation ($Contrast = 0.64$) and Pearson's coefficients ($Contrast = 0.16$) fail to discriminate between the two groups.

Method	Contrast	patient A		control group B	
		$D^A(Q)$	$\sigma_D^A(Q)$	$D^B(Q)$	$\sigma_D^B(Q)$
Kullback-Leibler	3.25	0.53	0.057	0.66	0.035
Mutual Information	1.42	3.12	0.222	3.38	0.023
Spearman Rank Order	0.64	1.43	0.012	1.42	0.004
Pearson's coefficient	0.16	1.42	0.016	1.42	0.003

Table 2: *Discrimination power between patient A (acute phase: first four EEG-recordings of patient A) and control group B expressed by the Contrast (see Eq. 9).*

From the linear perspective the EEG-recordings of the FLE-patient and the control group are undistinguishable and form in this sense a homogenous group.

4.2 Spatio-Temporal Characterization

The spatial structuring of the brain activity can be studied in more detail by means of the hierarchical clustering as introduced in section 3.3. The hierarchical tree shows the relation between the signals obtained at the several electrodes. Two states of patient A (figure 4: before seizure, figure 5: during seizure) and a typical example of the control group (figure 6) are shown. In the left panel the hierarchical tree is shown, while the right panel gives a two dimensional approximation of the cluster behavior. In general, an exact two-dimensional solution is not possible. The color coding of these representations is identical in all figures: Cluster depth is color coded by blue (loose cluster) over green, yellow to red (strong cluster).

The ultrametric distance of each branch can be read from the ordinate. Following from top to bottom in the left panel, the clustering becomes stronger, i.e. the items (time series) that belong to the same branch become more similar to each other. Comparison of the figures show significant differences in the spatial structuring. First of all, we can see that the clusters are in general deeper in the FLE-patient than in the reference cases, as already shown in the previous section. The deepest cluster, however, are formed by the signals obtained in the frontal area (i.e. FP1-FP2) and in the occipital area (i.e. O1 and O2). During seizure attack, the latter one is sometimes even the deepest cluster, as for instance in figure 5. In contrast, in the control group the cluster depth decreases from the frontal to the occipital area (see figure 6). In particular, the synchronization between the signals in O1 and O2 is rather poor in the reference cases, with respect to each other and with respect to the signals obtained at all other positions. Moreover, the aggregation level of O1 and O2 is very often at the highest ultrametric distance (see figure 6)

The typical representation in figure 6 shows that normally — and on average — one observes a clusterization, which reflects the geometrical placements quite well. The clusters are predominantly formed along lines connecting the front side with the rear side, e.g.: FP1-F3, F7-T3-T5, FZ-CZ. The synchronization between the hemispheres, which is clearly visible in all cases, falls off backwards. In patient A, we observe stronger clustering along horizontal lines, such as T6-O2-O1-T5, and a closer clustering between geometrical more distant locations as for instance between occipital-parietal and frontal areas.

This is demonstrated by the two-dimensional visualization of the cluster properties in the sequence of figure 7 (patient A) and figure 8 (control group). The images show the time-averaged cluster behavior in succeeding EEG recordings: Thus these visualizations represent the mean cluster properties of the corresponding EEG signals. The upper left image shows the situation in patient

A before treatment. The overall degree of synchronization is very high. After starting effective treatment with valproic acid and lamotrigine clinical symptoms and seizures improved slowly. Only after readjustment of therapy with higher doses of valproic acid and lamotrigine the cluster properties (lower panel) are getting similar to that of the control group. The lower right image is computed from an EEG recording after five weeks of effective treatment. Even if there are still some accentuation in the frontal area and in the occipital area, the two-dimensional visualization is hardly distinguishable from that of the control group.

5 Discussion

The purpose of this investigation is the quantitative spatio-temporal characterization of brain activity from standard multi-channel scalp EEG recordings in a child suffering from frontal lobe epilepsy in contrast to a control group of age matched children without active epilepsy. From a diagnostic point of view an appropriate measure is missed, which quantitatively characterizes the status of the patient within the interictal phases. Therefore, the main objective was rather the description of the background activity, which is unsuspicious in usual visual inspection than the investigation of pre-seizure, seizure or post-seizure effects, their known accompanying electroencephalographic signatures [28] or a prediction of seizures (see e.g. [2], [29], [30]).

The basic assumption of our approach is that the obvious increased synchronization level of the brain activity during attacks persists in a weakened form within interictal epochs, even if this is not easily seen by means of conventional EEG analysis. Since the state of vigilance also affects strongly synchronization of brain activity, e.g. sleep enhances synchronization, only periods with the pa-

tients in a comparable state (i.e. awake, same assessment of level of attention) are included in the analysis. To study epilepsy related synchronization in multichannel EEG recordings, we investigated the suitability of a number of different linear as well as information based correlation measures (e.g. mutual information, Kullback-Leibler distances). Spatio-temporal resolution of the derived measures is achieved in the framework of the subsequent hierarchical cluster analysis.

In the case study of the patient suffering from frontal lobe epilepsy we find, that the synchronization level is significantly increased during its clinical manifestation with respect to all individuals of the control group. Out of a number of methods in time and frequency domain, mutual information and Kullback-Leibler distances have the highest contrast between the control group and the interictal activity of the FLE patient. After successful medical suppression of the acute epileptic state the clinical picture still points to the presence of a frontal lobe syndrome. In consequence of a long term effective therapy these symptoms disappeared. In the course of the two year lasting follow up of the patient, the synchronization measures converge to the values obtained for the members of the control group.

In detail, just after starting the medical treatment we observe strong changes of the global measures with a clear tendency towards the range defined by the reference group. Within the first weeks, however, the global and local measures still differ significantly from that of the control group, albeit the visual EEG inspection gives no hints to abnormal characteristics of background activity. After a short period of an about two month lasting treatment the chosen measures are no more distinguishable from that of the healthy probands in a statistical sense. Our results suggest that the newly developed method could

yield an appropriate parameter for the evaluation of the patients response to anticonvulsive drug treatment, which is independent of classical epilepsy-related EEG features. From a clinical point of view, we found that the development of the derived parameters is in parallel with the process of the psychological normalization.

The interpretation of the spatial characteristics given by the detailed cluster representation of the brain activity is more difficult. As far as the frontal lobe areas are concerned, our method confirms significantly an enhanced synchronization between the most relevant surface locations (i.e. FP1-FP2). Nevertheless, so far our spatial reconstruction is not able to narrow down substantially the assumed focal area. The most surprising aspect of our results, however, is that we observe striking differences in the spatial structuring of the occipital region (O1-O2), compared to the control group. This anomaly is clearly present in our characterizations, independent of the used measures, but beforehand undetected by the conventional EEG analysis.
A further result of our investigation is that in the pathological case of frontal lobe epilepsy the synchronization levels along paths connecting the hemisphere are more pronounced with respect to the results of the control group. In the latter case we observe that the brain activity clusters along lines connecting frontal with rear (occipital) parts. This phenomenon, in our opinion, resembles the so called secondary bilateral synchrony (SBS), which is well known from literature ([31], [32]). SBS is frequently associated with a focus in the frontal lobes, but it is rather the result of a complex interaction of multiple foci as Blume and Pillay argue [32]. The presence of multiple foci in our patient could not be settled.

In our opinion, the presented method can be helpful to extract additional di-

agnostic information out of inconspicuous background activity. The detailed analysis of EEG signals from selected areas with the help of the shown cluster ansatz promises valuable and specific information on local synchronization features.
In general, we expect that the information gain of our approach benefits from a higher spatial and temporal resolution of the data.

As a related application of our approach, we see the study of neurodevelopmental disorders like autism. In this context Kulisek et al. [33] were able to characterize autistic children by means of synchronization levels.

References

[1] Singer W. Synchronization, Binding and Expectancy. In: Arbib MA, editor. The Handbook of Brain Theory and Neural Networks. MIT Press; 2003. p. 1136–1143.

[2] Jerger KK, Netoff TI, Francis JT, Sauer T, Pecora L, Weinstein SL, et al. Early Seizure Detection. Journal of Clinical Neurophysiology. 2001;18(3):259–268.

[3] Paluš M, Komárek V, Procházka T, Hrncír Z, Sterbová K. Synchronization and Information Flow in EEGs of Epileptic Patients. IEEE Engineering in Medicine and Biology Magazine. 2001 sep/oct;20(5):65–71.

[4] Hegde A, Erdogmus D, Shiau DS, Principe JC, Sackellares CJ. Clustering Approach to Quantify Long-Term Spatio-Temporal Interactions in Epileptic Intracranial Electroencephalography. Computational Intelligence and Neuroscience. 2007;p. 1–18. Article ID 83416, doi:10.1155/2007/83416.

[5] Pillai J, Sperling MR. Interictal EEG and the Diagnosis of Epilepsy. Epilepsia. 2006;47, Suppl 1:14–22.

[6] Fingelkurts AA, Fingelkurts AA, Kaplan AY. Interictal EEG as a Physiological Adaptation. Part I. Composition of Brain Oscillations in Interictal EEG. Clinical Neurophysiology. 2006;117:208–222.

[7] Aso K, Watanabe K, Negoro T, Nakashima S. Frontal Lobe Epilepsy of Childhood Onset. Epilepsia. 1997;38(Suppl. 6):40–41.

[8] Salanova V, Morris HH, Ness PV, Kotagal P, Wyllie E, Lüders H. Frontal Lobe Seizures: Electroclinical Syndromes. Epilepsia. 1995 Jan;36(1):16–24.

[9] Fusco L, Iani C, Faedda MT, Manfredi M, Vigevano F, Ambrosetto G. Mesial Frontal-Lobe Epilepsy: a Clinical Entity not Sufficiently Described. Journal of Epilepsy. 1990;3(3):123–135.

[10] Lüders HO, Burgess R, Noachtar S. Expanding the International Classification of Seizures to Provide Localization Information. Neurology. 1993 Sep;43(9):1650–1655.

[11] Kotagal P, Lüders HO, Williams G, Nichols TR, McPherson J. Psychomotor Seizures of temporal Lobe Onset: Analysis of Symptom Clusters and Sequences. Epilepsy Research. 1995;20:49–67.

[12] Fohlen M, Bulteau C, Jalin C, Jambaque I, Delalande O. Behavioural Epileptic Seizures: A Clinical and Intracranial EEG Study in 8 Children with Frontal Lobe Epilepsy. Neuropediatrics. 2004 Dec;35(6):336–345.

[13] Kellinghaus C, Lüders HO. Frontal Lobe Epilepsy. Epileptic Disorders. 2004 Dec;6(4):223–239.

[14] Riva D, Avanzini G, Franceschetti S, Nichelli F, Saletti V, Vago C, et al. Unilateral Frontal Lobe Epilepsy Affects Executive Functions in Children. Neurological Sciences. 2005;26:263–270.

[15] Elger CE, Brockhaus A, Lendt M, Kowalik A, Steidele S. Behavior and Cognition in Children with Temporal Lobe Epilepsy. In: Tuxhorn I, Holthausen H, Boeingk HE, editors. Pediatric Epilepsy Syndromes and their Surgical Treatment. London-Paris-Rome: John Libbey; 1995. .

[16] Harvey AS, Berkovic SF, Wrennall JA, Hopkins IJ. Temporal Lobe Epilepsy in Childhood: Clinical, EEG, and Neuroimaging Findings and Syndrome Classification in a Cohort with New-Onset Seizures. Neurology. 1997;49(4):960–968.

[17] Manford M, Fish DR, Shorvon SD. An Analysis of Clinical Seizure Patterns and their Localizing Value in Frontal and Temporal Lobe Epilepsies. Brain. 1996;119(1):17–40.

[18] Bonanno G, Lillo F, Mantegna RN. High-frequency cross-correlation in a set of stocks. Quantitative Finance. 2001;1:96–104.

[19] Aschenbrenner T, Springer S, Bunk W. Therapiebedingte Änderung der raumzeitlichen Strukturierung des Oberflächen-EEG bei Kindern mit Frontallappenepilepsie. Zeitschrift für Epileptologie. 2005 May;18(2):141.

[20] Lee U, Kim S, Jung KY. Classification of Epilepsy Types Through Global Network Analysis of Scalp Electroencephalograms. Physical Review E. 2006;73:041920–1–041920–9.

[21] Kullback S, Leibler RA. On Information and Sufficiency. The Annals of Mathematical Statistics. 1951;22(1):79–86.

[22] Johnson DH, Sinanović S. Symmetrizing the Kullback-Leibler Distance; 2001. http://citeseer.ist.psu.edu/johnson01symmetrizing.html.

[23] Legendre P, Legendre L. Numerical Ecology. vol. 20 of Developments in Environmental Modelling. 2nd ed. Elsevier; 1998.

[24] Gower JC, Ross GJS. Minimum Spanning Tree and Single Linkage Cluster Analysis. Applied Statistics. 1969;18(1):54–64.

[25] Rammal R, Toulouse G, Virasoro MA. Ultrametricity for physicists. Reviews of Modern Physics. 1986;58(3):765–788.

[26] Kruskal JB. On the Shortest Spanning Subtree of a Graph and the Traveling Salesman Problem. Proceedings of the American Mathematical Society. 1956;7:48–50.

[27] Prim RC. Shortest Connection Networks and some Generalizations. The Bell System Technical Journal. 1957;36(6):1389–1401.

[28] Meier R, Dittrich H, Schulze-Bonhage A, Aertsen A. Detecting Epileptic Seizures in Long-Term Human EEG: A New Approach to Automatic Online and Real-Time Detection and Classification of Polymorphic Seizure Patterns. Journal of Clinical Neurophysiology. 2008 Jun;25(3):1–13.

[29] Quyen MLV, Martinerie J, Navarro V, Boon P, D'Havé M, Adam C, et al. Anticipation of Epileptic Seizures from Standard EEG Recordings. The Lancet. 2001 Jan 20;357:183–188.

[30] Navarro V, Martinerie J, Quyen MLV, Baulac M, Dubeau F, Gotman J. Seizure Anticipation: Do Mathematical Measures Correlate with Video-EEG Evaluation? Epilepsia. 2005;46(3):385–396.

[31] Tükel K, Jasper H. The Electroencephalogram in Parasagittal Lesions. Electroencephalography and Clinical Neurophysiology. 1952;4:481–494.

[32] Blume WT, Pillay N. Electrographic and Clinical Correlates of Secondary Bilateral Synchrony. Epilepsia. 1985;26(6):636–641.

[33] Kulisek R, Hrncir Z, Hrdlicka M, Faladova L, Sterbova K, Krsek P, et al. Nonlinear Analysis of the Sleep EEG in Children with Pervasive Developmental Disorder. Neuro Endocrinology Letters. 2008;29(4):512–517.

List of Figure Legends:

1. *Time course of the mean distance* $D(M_t)$ *— based on the mutual information — for the second EEG recording of patient A (age=* $12.10\ yr$*). The according value of the averaged mean distance* $D(M_t) = 3.103$ *and standard deviation* $\sigma_D(M_t) = 0.075$ *(compare second observation of patient A in figure 3). At about* $6.7\ min$ *an epileptic seizure (hatched area) starts. The seizure attack is initiated by a loss of synchronization, while during the seizure the correlation is generally increased, thus the distance values are low. The red horizontal lines mark the mean value and standard deviation of the different EEG recordings of patient A. The blue horizontal lines label the corresponding quantities for the control group. Periods with interictal epileptiform discharges or ictal patterns, labeled in gray, are eliminated and do not enter the statistics.*

2. *Mean Kullback-Leibler distance for patient A (acute phase: red, non-acute phase: green) and control group (blue) of the power spectra. The filled circles denote the averaged mean Kullback-Leibler distance* $D(E)$*, the error bars indicate the range* $\pm\sigma_D(E)$ *of the single EEG recordings. The horizontal lines label the mean Kullback-Leibler distance for patient A and control group, the dashed lines label the respective standard deviations.*

3. *Mean mutual Information for patient A (acute phase: red, non-acute phase: green) and control group (blue). The filled circles denote the averaged mean mutual information* $D(M)$*, the error bars indicate the standard deviations* $\sigma_D(M)$ *of the single EEG recordings. The horizontal lines label the mean mutual information for patient A and control group, the dashed lines mark the respective standard deviations.*

4. *Spatio-temporal characteristic of brain activity based on mutual information of patient A before seizure (see figure 1). This EEG recording correspond to A2*

in figure 7. The left panel shows the exact clustering scheme expressed by an hierarchical tree (labeled in red: FP1, FP2, O1, O2) while on the right side a two-dimensional approximation is presented.

5. *Spatio-temporal characteristic of brain activity based on mutual information of patient A during seizure (see figure 1). This EEG recording correspond to A2 in figure 7.*

6. *Representative example of spatio-temporal characteristic of brain activity based on mutual information from control group. This EEG recording correspond to B1 (sixth EEG, age 11.86 y) in figure 8. In general, cluster depth decreases from the frontal to the occipital area.*

7. *Change of mean spatio-temporal structuring of brain activity based on mutual information in patient A reflecting the change of clinical features under therapy. A1 to A4 refers to the first four EEG of patient A ordered by age (see table 1, figure 2 or 3): A1 12.06 y, A2 12.10 y, A3 12.10 y, A4 12.16 y. The color coding is identical to that used in figures 4–6. Patient A exhibit strong clustering along horizontal lines and close clustering between geometrical more distant locations as for instance between occipital-parietal and frontal areas.*

8. *Representative examples of mean spatio-temporal structuring of brain activity based on mutual information in control group. B1 to B4 refers to the EEG of the control group ordered by age (see table 1, figure 2, 3 and 6): B2 11.28 y, B1 11.32 y (fifth EEG), B1 11.86 y (sixth EEG), B4 14.37 y. Brain activity in the control group clusters predominantly along the frontal-occipital direction with decreasing cluster strength. The color coding is identical to that used in figures 4–7.*

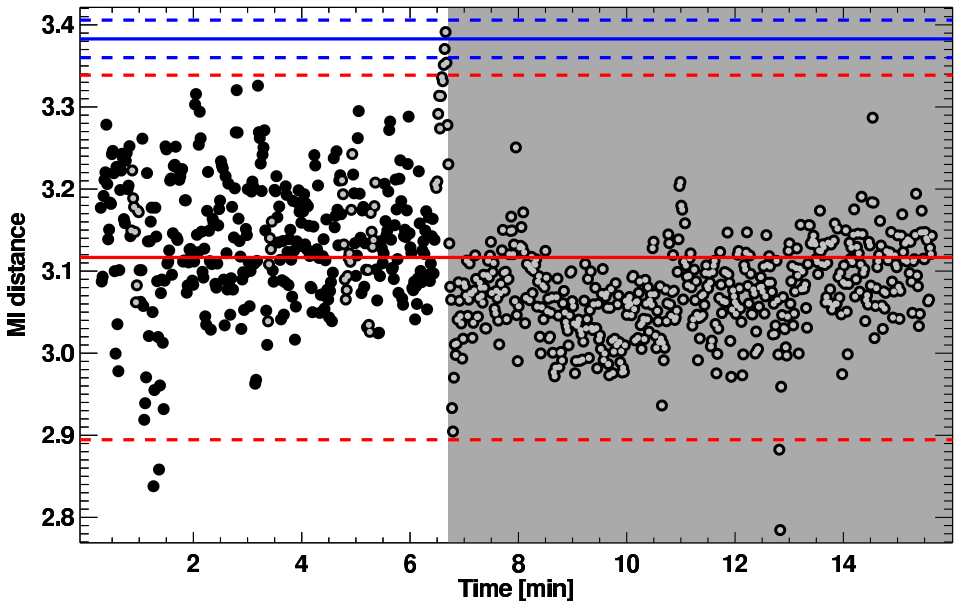

Figure 1: *Time course of the mean distance $D(M_t)$ — based on the mutual information — for the second EEG recording of patient A (age= 12.10 yr). The according value of the averaged mean distance $D(M_t) = 3.103$ and standard deviation $\sigma_D(M_t) = 0.075$ (compare second observation of patient A in figure 3). At about 6.7 min an epileptic seizure (hatched area) starts. The seizure attack is initiated by a loss of synchronization, while during the seizure the correlation is generally increased, thus the distance values are low. The red horizontal lines mark the mean value and standard deviation of the different EEG recordings of patient A. The blue horizontal lines label the corresponding quantities for the control group. Periods with interictal epileptiform discharges or ictal patterns, labeled in gray, are eliminated and do not enter the statistics.*

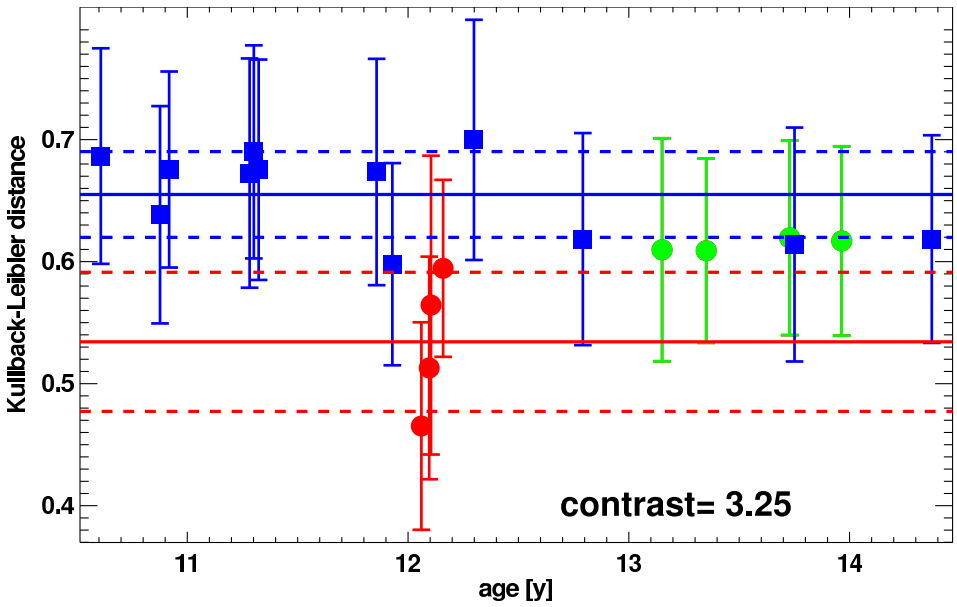

Figure 2: *Mean Kullback-Leibler distance for patient A (acute phase: red, non-acute phase: green) and control group (blue) of the power spectra. The filled circles denote the averaged mean Kullback-Leibler distance $D(E)$, the error bars indicate the range $\pm\sigma_D(E)$ of the single EEG recordings. The horizontal lines label the mean Kullback-Leibler distance for patient A and control group, the dashed lines label the respective standard deviations.*

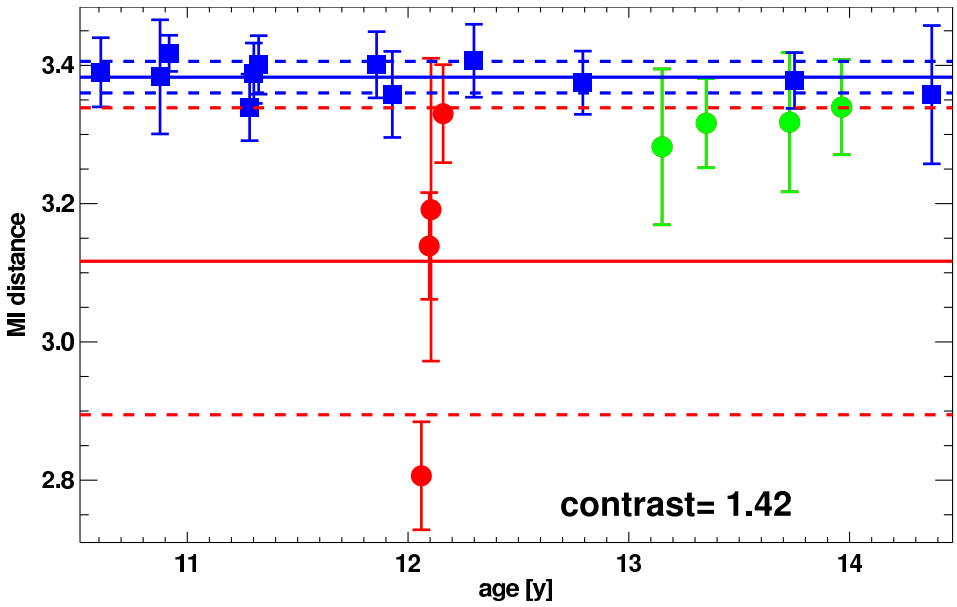

Figure 3: *Mean mutual Information for patient A (acute phase: red, non-acute phase: green) and control group (blue). The filled circles denote the averaged mean mutual information $D(M)$, the error bars indicate the standard deviations $\sigma_D(M)$ of the single EEG recordings. The horizontal lines label the mean mutual information for patient A and control group, the dashed lines mark the respective standard deviations.*

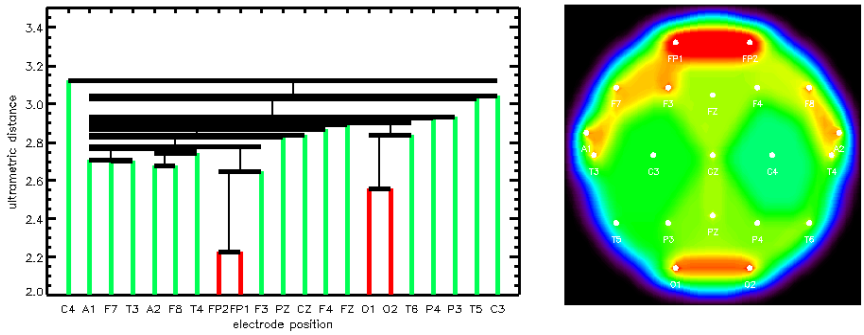

Figure 4: *Spatio-temporal characteristic of brain activity based on mutual information of patient A before seizure (see figure 1). This EEG recording correspond to A2 in figure 7. The left panel shows the exact clustering scheme expressed by an hierarchical tree (labeled in red: FP1, FP2, O1, O2) while on the right side a two-dimensional approximation is presented.*

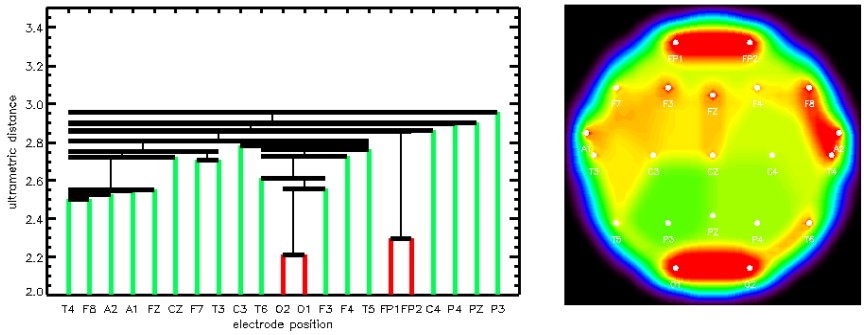

Figure 5: *Spatio-temporal characteristic of brain activity based on mutual information of patient A during seizure (see figure 1). This EEG recording correspond to A2 in figure 7.*

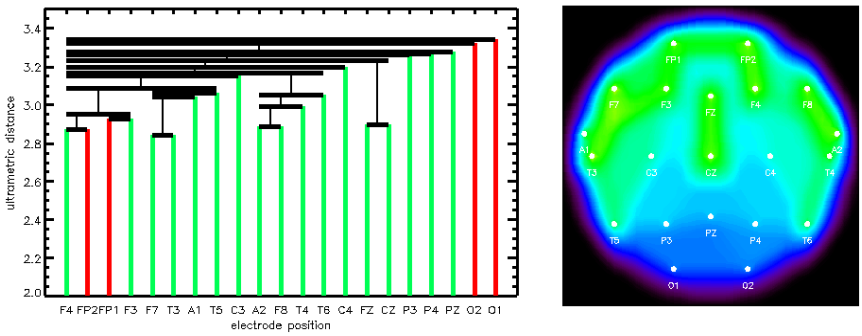

Figure 6: *Representative example of spatio-temporal characteristic of brain activity based on mutual information from control group. This EEG recording correspond to B1 (sixth EEG, age 11.86 y) in figure 8. In general, cluster depth decreases from the frontal to the occipital area.*

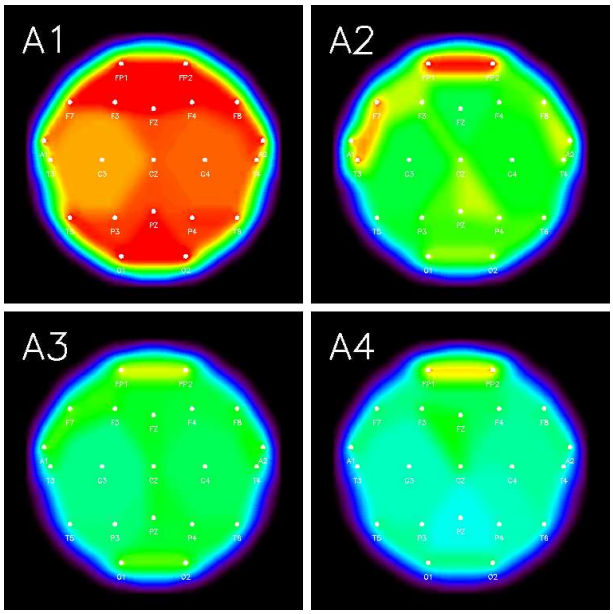

Figure 7: *Change of mean spatio-temporal structuring of brain activity based on mutual information in patient A reflecting the change of clinical features under therapy. A1 to A4 refers to the first four EEG of patient A ordered by age (see table 1, figure 2 or 3): A1 12.06 y, A2 12.10 y, A3 12.10 y, A4 12.16 y. The color coding is identical to that used in figures 4–6. Patient A exhibit strong clustering along horizontal lines and close clustering between geometrical more distant locations as for instance between occipital-parietal and frontal areas.*

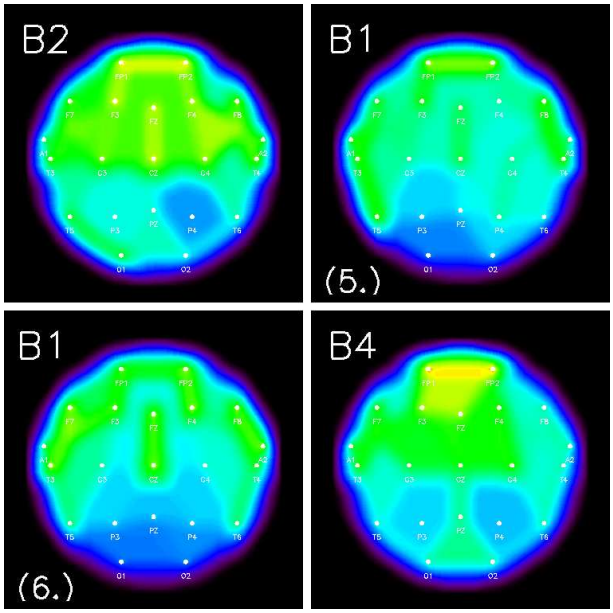

Figure 8: *Representative examples of mean spatio-temporal structuring of brain activity based on mutual information in control group. B1 to B4 refers to the EEG of the control group ordered by age (see table 1, figure 2, 3 and 6): B2 11.28 y, B1 11.32 y (fifth EEG), B1 11.86 y (sixth EEG), B4 14.37 y. Brain activity in the control group clusters predominantly along the frontal-occipital direction with decreasing cluster strength. The color coding is identical to that used in figures 4–7.*